LANGMUIR Article
Cite This: Langmuir 2019, 35, 2283−2288
pubs.acs.org/Langmuir

Sol−Gel Coexisting Phase of Polymer Microgels Triggers Spontaneous Buckling

Keisuke Koyanagi,[†] Kazue Kudo,[‡] and Miho Yanagisawa*[,†,§,∥]

[†]Department of Applied Physics, Tokyo University of Agriculture and Technology, Naka-cho 2-24-16, Koganei, Tokyo 184-8588, Japan

[‡]Department of Computer Science, Ochanomizu University, Otsuka 2-1-1, Bunkyo, Tokyo 112-8610, Japan

[§]Department of Basic Science and [∥]Komaba Institute for Science, The University of Tokyo, Komaba 3-8-1, Meguro, Tokyo 153-8902, Japan

Supporting Information

ABSTRACT: Mechanical buckling is a ubiquitous phenomenon of elastic bodies like core−shell microgels. Although conventional theory predicts that sufficiently high pressure is the primary factor inducing the buckling of core−shell microgels, they often buckle spontaneously without applying pressure. We explored such spontaneous buckling of microgels by introducing interfacial tension between the gel phase of the shell and sol phase of the core. Thus, we found that the core−shell microgels in a sol−gel coexisting phase with a certain shell thickness ratio exhibit spontaneous buckling. According to our theoretical analysis, spontaneous buckling occurs due to the balance between the gel elasticity E and interfacial tension γ when the characteristic length γ/E is comparable to the microgel size R. Moreover, we found that the ratio between γ/E and R determines the buckling condition of the shell thickness ratio. Our findings establish an important framework for applying spontaneous buckling to the shape control of elastic bodies.

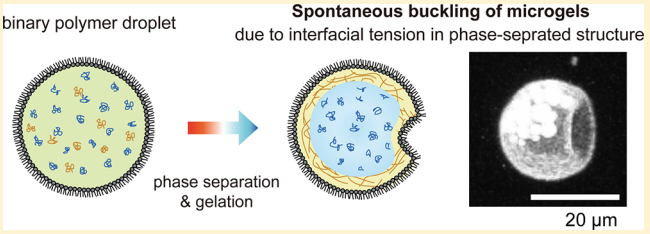

INTRODUCTION

Wrinkling in elastic bodies such as fruits, vegetables, biological tissues, and polymer gels is known to be related to the buckling phenomenon caused by mechanical instability on the surface.[1−3] The buckling phenomenon attracts much attention for numerous applications such as tunable surface fabrication,[4−7] optics,[8−10] bioengineering,[11] stretchable electronics,[12,13] and mechanical measurements.[14]

Compared to stress-driven buckling (constrained swelling in response to environmental stimuli), pressure-driven buckling exhibits a simpler mechanism: buckling occurs when the external pressure exceeds a critical pressure P_c. In the case of a spherical shell with an outer radius R and a shell thickness h, the value of P_c is described by using two parameters: (i) the shell thickness ratio, h/R, and (ii) the Young's modulus of the shell, E, as follows:[15−17]

$$P_c = \frac{2E}{\sqrt{3(1-\mu^2)}}\left(\frac{h}{R-\frac{h}{2}}\right)^2 \quad (1)$$

where μ is Poisson's ratio of the elastic shell.

Although elastic bodies show buckling under a sufficiently large pressure, the critical pressure at which buckling occurs is often lower than the theoretical value. In the case of spherical shells of polymer gels (core−shell microgels), one of the reasons is the inhomogeneity of the elastic shells. The influence of spatially varying thickness h and elasticity E on the buckling mechanism of the shell has been investigated experimentally[18] and theoretically.[19] Another reason is inhomogeneity in the internal structure of the elastic bodies. Spherical microgels prepared from emulsion polymerization often buckle spontaneously without applying pressure.[20−23] Sacanna et al. explained that spontaneous buckling might occur when the remaining polymer polymerizes inside previously cross-linked spherical shells.[20,21] This indicates that the inhomogeneous internal structure of microgels in the sol−gel coexisting phase plays an important role in the spontaneous buckling. However, how the sol−gel coexisting phase in elastic bodies causes the buckling is still elusive.

Here, we aimed to elucidate the underlying mechanism by which the inhomogeneous internal structure of polymer gels in a sol−gel coexisting phase causes spontaneous buckling without applying pressure. For this purpose, we used core−shell microgels prepared from phase separation solutions of poly(ethylene glycol) (PEG) and gelatin confined within lipid droplets.[24] The gelatin/PEG system enabled us to regulate the sol−gel coexisting phase by changing the quenching rate because both phase separation with complete wetting of gelatin on the lipid membrane and gelation of the gelatin proceed with a decrease in temperature.[24−26] We demonstrated that the interfacial tension between the gel phase of the shell and sol

Received: November 6, 2018
Revised: December 18, 2018
Published: January 14, 2019

DOI: 10.1021/acs.langmuir.8b03751
Langmuir 2019, 35, 2283−2288

phase of the core is responsible for the spontaneous buckling of the core−shell microgels. Our theoretical analysis reveals that spontaneous buckling occurs due to the balance between the gel elasticity and interfacial tension when the characteristic length is comparable to the microgel size. Our findings provide new insights into the mechanism by which the inhomogeneous internal structure of elastic bodies causes buckling during polymerization[20−23,27,28] and phase separation.[29,30]

EXPERIMENTAL SECTION

Materials. 1,2-Dioleoyl-*sn*-glycero-3-phosphoethanolamine (PE) was purchased from Wako Pure Chemical Industries (Osaka, Japan). Mineral oil was purchased from Nacalai Tesque (Kyoto, Japan), while alkali-treated gelatin was supplied by Merck (Darmstadt, Germany). The average molecular weight determined by gel permeation chromatography was 69000. Poly(ethylene glycol) (molecular weight 1000; PEG 1k) was purchased from Sigma-Aldrich. Thioflavin T (ThT; Wako) and fluorescein isothiocyanate isomer I (FITC; Sigma-Aldrich Japan; Tokyo, Japan) were used as a fluorescent dye for the gelatin-rich gel phase. All the materials were used without further purification.

Preparation of Core−Shell Microgels. For preparing core−shell microgels, we confined a gelatin/PEG solution inside lipid droplets in oil. The gelatin/PEG solution underwent phase separation and gelation with a decrease in temperature (Figure 1a). The droplets were coated

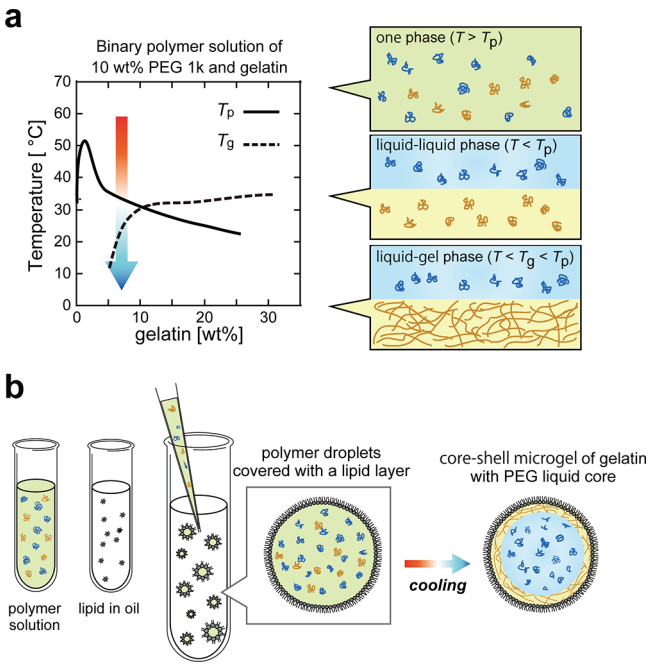

Figure 1. (a) Schematic illustrations of (left) phase diagram of 10 wt % PEG 1k and various concentrations of gelatin and of (right) three different phases appeared with a decrease in temperature along the arrow. The solid and dashed lines indicate the phase separation point T_p and the gelation point T_g, respectively. (b) Preparation of core−shell microgels. Above T_p, the gelatin/PEG solution was entrapped in lipid-coated droplets via pipetting. After the cooling, the gelatin/PEG droplets transit to core−shell microgel of gelatin with PEG liquid core.

with a lipid layer in an oil phase. First, dry films of the lipid PE formed at the bottom of a glass tube. The mineral oil was added to the lipid films followed by 90 min of sonication. The final concentration of the lipid/oil solution was ∼1 mM. The gelatin and PEG 1k were dissolved in water at 70 °C (above the gelation temperature T_g and phase separation temperature T_p: Figure 1a) for 1 h. To prepare droplets, a binary polymer solution of 10 wt % PEG 1k and 9 wt % gelatin was added to the lipid/oil solution at 70 °C and emulsified via pipetting. We placed an aliquot containing the droplets on a silicone-coated cover glass to prevent the droplets from sticking to the glass plate. Owing to the temperature quenching below T_p and T_g, the gelatin/PEG droplets transited to core−shell microgels, as reported previously[24] (Figure 1b).

Fluorescence Observation of Microgels. The microgels were observed by fluorescence microscopy (Olympus IX81; Olympus) and confocal laser scanning fluorescence microscopy (CLSM) (Olympus IX83 with FV1200). Fluorescent images of fluorescein-tagged gelatin and thioflavin (ThT), which were excited by a mercury lamp or laser at 488 nm, were obtained using fluorescence filter sets (U-FBNA and U-MNIBA3; from 510 to 550 nm). The sample was cooled from 70 to 4 °C (below T_g) at a rate of ∼0.01−40 °C/min using a Peltier-type cooling heating stage (10021, Linkam; Scientific Instruments, Ltd., UK). The pinhole size was fixed to be 1 μm. The obtained images were analyzed by "National Institutes of Health ImageJ" software.

RESULTS AND DISCUSSION

Buckling of Core−Shell Microgels in Sol−Gel Coexisting Phase. To regulate the inhomogeneous internal structure of microgels in the coexisting sol−gel phase, we prepared core−shell microgels from gelatin/PEG droplets. The gelatin/PEG solution simultaneously caused phase separation and gelation with a decrease in temperature (Figure 1a). For 10 wt % PEG 1k and 9 wt % gelatin solutions, the phase separation temperature T_p was slightly higher than the gelation temperature T_g. Upon temperature quenching, the one-phase gelatin/PEG solution first separated into two liquid phases below T_p, following which the gelatin-rich phase turned into a gel phase below T_g.[31] The higher quenching rate prevented coarsening from the earlier stage of phase separation upon gelation. By changing the quenching rate for the gelatin/PEG solution with $T_p > T_g$, we regulated the inhomogeneity derived from the coexisting sol−gel phase.

The gelatin/PEG solution in one phase (at above T_p) was confined inside the droplets covered with a lipid layer of phosphatidylethanolamine (PE) (Figure 1b). The radius of the obtained droplets was in the range 5−50 μm. Given that gelatin has a high affinity for a PE membrane compared to PEG, the gelatin-rich phase localized near the droplet PE surface and finally formed a spherical shell of gelatin gel with the PEG solution at the core, as reported previously.[24]

To modify the inner structure of the core−shell microgels, we increased the temperature quenching rate from 70 to 4 °C (from above T_p to below T_g) to 0.1 to 50 °C/min. Under a certain quenching rate, the gelatin/PEG microgels underwent a sudden buckling transition without applying pressure (Movie S1). Figure 2a (left) shows a differential interference contrast (DIC) image of a buckling microgel. The buckling microgels quickly recovered the initial spherical shape upon temperature increase above T_g (Figure 2a (right) and Movie S2). When the temperature quenched below T_g, the microgels buckled again (Movie S1 shows the second buckling). This means that the observed buckling is a reversible phenomenon caused by the temperature change across T_g. The reversible buckling is due to the inner coexisting phase of the microgel which reversibly changes with temperature shift. The overall size of the buckling microgels was similar to the initial size of spherical droplets at above T_p. Hereinafter, the outer radii (R) of the droplet in the liquid phase and the microgel in the sol−gel phase are identical. Such buckling of microgels and volume change by temperature quenching were not observed for homogeneous microgels of gelatin without PEG (Figure S1).

By visualizing the inhomogeneous inner structure of the microgels,[32] we obtained cross-sectional images and three-

DOI: 10.1021/acs.langmuir.8b03751
Langmuir 2019, 35, 2283−2288

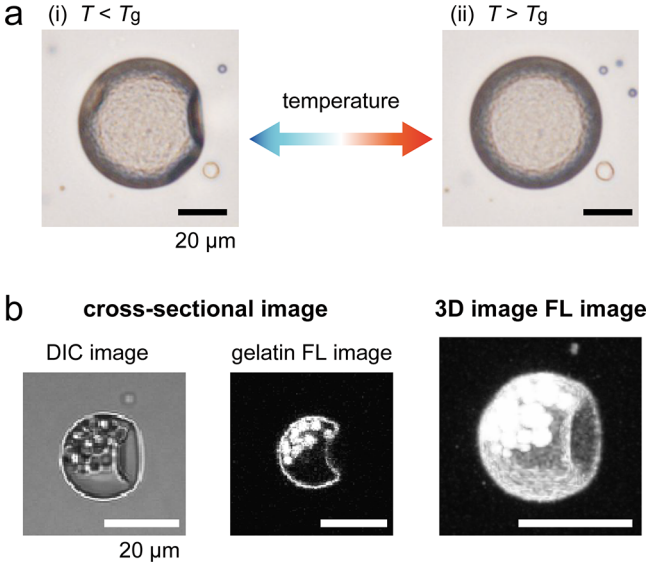

Figure 2. (a) Reversible buckling phenomena by changing temperature across the phase separation temperature and the gelation temperature T_g ($<T_p$). (b) An example of buckling microgels is shown as the DIC image (left), confocal cross-sectional fluorescence (FL) image of the gelatin-rich phase (center), and the 3D FL image (right).

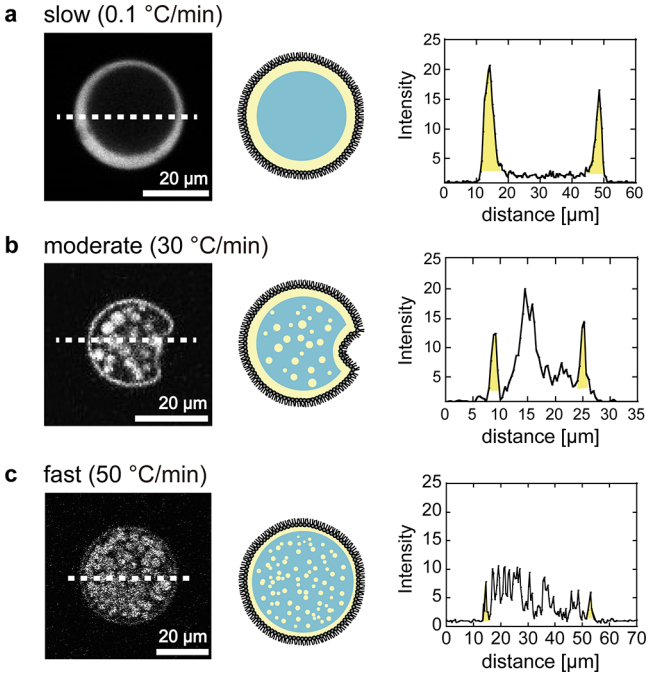

Figure 3. Quench rate dependence of buckling of core−shell microgels and the shell thickness. An example of gelatin/PEG microgels is shown as confocal cross-sectional fluorescence (FL) image of gelatin-rich phase (left) and the schematic image (center). The gelatin-rich gel phase and PEG-rich liquid phase are shown in white (yellow) and black (blue), respectively. (right) Intensity profiles along the dotted lines in the FL images. The yellow regions correspond to the shell of gelatin gel.

dimensional (3D) images of the buckling microgels with a fluorescent dye for the gelatin-rich phase, namely Thioflavin T (ThT) (Figure 2b). We confirmed that the ThT was localized and visualized in the gelatin-rich phase, like FITC-conjugated gelatin (Figure S2). The gelatin-rich phase formed core−shell microgels with the PEG solution at the core. Given that the thickness of the shell was spatially uniform, this buckling was not caused by the stress concentration on the thin part of the inhomogeneous shell. The most possible trigger for spontaneous buckling is the inhomogeneous inner structure in the sol−gel coexisting phase upon gelatin during phase separation.

Inhomogeneous Inner Structure of Buckling Microgels. To clarify the relation between the quenching rate and internal structure of the buckling microgels, the fluorescence images of the microgels were compared for several conditions associated with different quenching rates. When the quenching rate is low enough to complete phase separation into two liquid phases before gelation, a thick shell capsule is obtained, as depicted in Figure 3a (low quenching rate, 0.1 °C/min). Under this condition, the shell thickness is 2 μm < h < 7 μm for droplets with 5 μm < R < 50 μm, which corresponds to the h value estimated from the volume fraction of the gelatin-rich phase (30−45 vol %). With an increase in the quenching rate up to 30 °C/min (moderate quenching rate, Figure 3b), we observed spontaneous buckling of microgels. The shells of the buckling microgels were thinner than those of microgels for the low quenching rate because the gelation prevented coarsening from the initial stage of phase separation. Resultant domains of the gelatin-rich phase formed isolated domains inside the gelatin capsules without coalescence with the capsule wall. For a high quenching rate (50 °C/min), the shell was much thinner, as shown in Figure 3c ($h \ll 0.8$ μm). In the fast quenching condition, buckling was not observed, as was the case with the slow quenching condition. These results clearly show that the spontaneous buckling condition of the shell thickness has an adequate value.

To clarify the spontaneous buckling condition of the shell thickness h, the h of microgels with and without buckling is plotted against the microgel size R in Figure 4a. The quenching rate is 30 °C/min (moderate quenching rate). It clearly demonstrates that buckling is not observed for core−shell

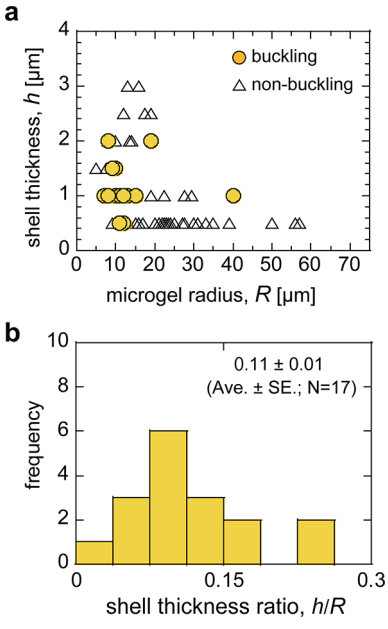

Figure 4. (a) Microgel size R dependence of shell thickness h for buckling core−shell microgels (closed yellow circles) and for nonbuckling core−shell microgels (triangles). (b) Histogram of shell thickness ratio, h/R, for buckling core−shell microgels.

DOI: 10.1021/acs.langmuir.8b03751
Langmuir 2019, 35, 2283−2288

microgels with large shell thickness ($h > 2.5\ \mu$m) and with small shell thickness ($h \ll 1\ \mu$m). Only microgels with medium shell thickness (average ± SE = 1.2 ± 0.2; $N = 17$) exhibit buckling. Moreover, small microgels ($R = 12.5 \pm 1.9\ \mu$m; $R_{min} = 7\ \mu$m) seem more likely to buckle than large microgels ($R \gg 20\ \mu$m), and the reduced volume of such buckling microgels is increased up to 40 vol % (Figure S3). Compared to localized buckling with the large reduced volume, the presence of slight buckling at the surface is difficult to judge, especially for small microgels. This may be the reason that buckling and nonbuckling microgels seem to coexist under the same shell thickness and microgel radius conditions. The histogram of the shell thickness ratio h/R has a peak, as shown in Figure 4b (0.11 ± 0.01 (average ± SE)). In the conventional buckling theory (eq 1), pressure-induced buckling under a constant pressure is observed for spherical shells with a smaller shell thickness ratio than a certain value. Therefore, the existence of a lower limit for h/R constitutes a unique condition for the spontaneous buckling of microgels in the sol−gel coexisting phase.

Mechanism of Spontaneous Buckling for Core−Shell Microgels. To explain the observed spontaneous buckling without applying pressure, we calculated the force balance for core−shell microgels with a liquid core. The extended critical pressure P should be composed of two factors: gel elasticity P_c (eq 1) and interfacial tension P_{int} as illustrated in Figure 5a.

$$P = P_c - P_{int} = \frac{2E}{\sqrt{3(1-\mu^2)}}\left(\frac{h}{R-\frac{h}{2}}\right)^2 - \frac{2\gamma}{R-h} \tag{2}$$

where E, μ, and γ are the Young's modulus of the shell in the gel phase, Poisson's ratio of the elastic shell, and interfacial tension between gel phase at the skin shell (gelatin-rich phase) and sol phase at the core (PEG-rich phase), respectively. These values of P_c and $-P_{int}$ are plotted against the shell thickness ratio h/R in Figure 5b, where E, μ, R, and γ are fixed to 100 Pa, 0.5, 10 μm, and 100 μN/m, respectively.[26,32] With an increase in h/R, the P_c increases as well, whereas $-P_{int}$ decreases, because the surface area at the phase interface becomes smaller. Therefore, the extended critical pressure P ($= P_c - P_{int}$) becomes a downward-convex function of h/R depending on the values of E and γ.

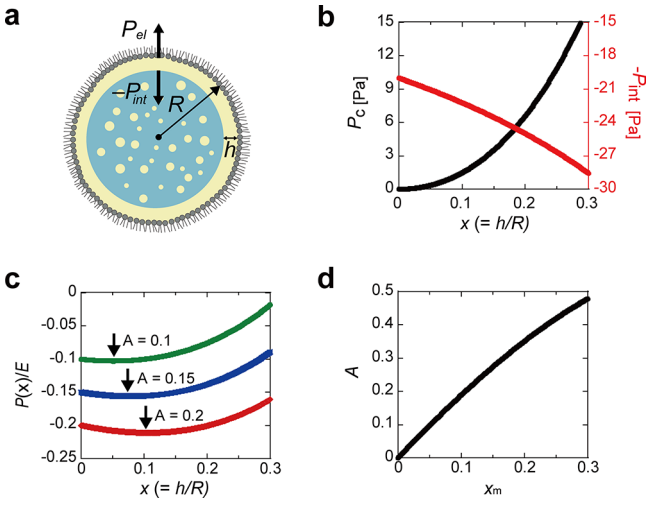

Figure 5. (a) Schematic illustration of force balance between elastic pressure P_c and interfacial tension pressure $-P_{int}$. R and h denote the outer radius of the core−shell microgel and shell thickness of the gel capsule (yellow). (b) Values of P_c and $-P_{int}$ are plotted against the shell thickness ratio h/R. The values of E, γ, R, and μ are 100 Pa, 100 μN/m, 10 μm, and 0.5, respectively. (c) Normalized extended critical pressure $P(x)/E$ ($= (P_c - P_{int})/E$) with various A ($= 2\gamma/ER$) is plotted against the shell thickness ratio, x ($= h/R$). The allows to denote the minimum points. (d) The relation between the A and the x value at the minimum point, x_m.

In our experimental results, the core−shell microgels show spontaneous buckling when h/R reaches a certain value (h/R = 0.11 ± 0.01; see Figure 4b). We interpret this in terms of the extended critical pressure P of a downward-convex function reaching a minimum at a certain h/R value ($h/R = 0.11$) and the core−shell microgels having that h/R value tending to buckle more easily than microgels having smaller and larger values of h/R.

To derive the condition of P with a minimum point, we rewrite eq 2 as a function of h/R ($\equiv x$) as follows:

$$\frac{P(x)}{E} = \frac{2}{\sqrt{3(1-\mu^2)}}\left(\frac{x}{1-\frac{x}{2}}\right)^2 - \frac{A}{1-x} \tag{3}$$

$$A \equiv \frac{2\gamma}{ER} \tag{4}$$

We plot $P(x)/E$ for various A in Figure 5c. Depending on the value of A, the minimum point of $P(x)$ changes, and its x value increases with A. The relation between the parameter A and x value at the minimum point, x_m, is derived from eq 3 as follows:

$$A = \frac{2}{\sqrt{3(1-\mu^2)}}\frac{x_m(1-x_m)^2}{\left(1-\frac{x_m}{2}\right)^3} \tag{5}$$

Thus, the parameter A has a positive correlation with the shell thickness ratio x_m. The value of A is plotted against x_m under the experimental condition ($x < 0.3$) in Figure 5d. It shows that the value of A should be smaller than 0.5 for $P(x)$ to have a minimum point.

We assume that the ratio γ/E is independent of the microgel size R because the confined polymer composition is independent of the confined size R. Figure 5d shows that the value of A ($= 2\gamma/ER$), which is a decreasing function of R, increases with increasing x_m at the minimum point of $P(x)$. Therefore, we expect that a larger buckling microgel has a smaller shell thickness ratio; i.e., h/R at the minimum point is a decreasing function of R. To verify this, we plot them as shown in Figure 6 (closed circles; by using the data in Figure 4a) and fit the data with eq 6, rewriting eq 5 to R:

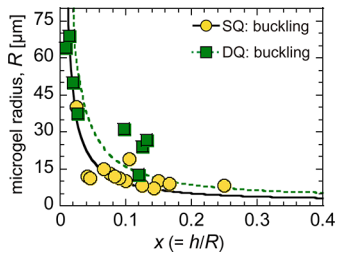

Figure 6. Relation between the size R of buckling microgels and the shell thickness ratio h/R for single quenching (SQ; circles) and double quenching with 10−30 min incubation time at T_p (DQ; squares). The solid and dashed lines are the fitting lines of eq 6 for SQ and DQ, respectively.

DOI: 10.1021/acs.langmuir.8b03751
Langmuir 2019, 35, 2283−2288

$$R = \frac{\gamma\sqrt{3(1-\mu^2)}}{E}\frac{\left(1-\frac{x_m}{2}\right)^3}{x_m(1-x_m)^2} \quad (6)$$

Figure 6 clearly demonstrates that the relation between h/R and R of the buckling microgels satisfies the theoretically obtained relation of eq 6. After fitting with μ fixed at 0.5, we found that the characteristic length γ/E is ∼0.6 μm.

Furthermore, Figure 5d suggests that the h/R of buckling microgels increases when increasing γ/E for fixed R conditions because A (= $2\gamma/ER$) is an increasing function of h/R. To change the value of γ/E, we performed double-quenching experiments where the sample was incubated for 10−30 min at the phase separation point T_p before the second quenching below the gelation point T_g occurred. As phase separation proceeded with an incubation process above T_g, we expected that the value of γ/E became greater than that of the single quenching experiment. This is because the interfacial tension γ increases until the progress of phase separation is inhibited by gelation. As plotted in Figure 6 (closed square), the h/R of buckling microgels with similar R for the double quenching was greater than that for single quenching. The fitting-derived γ/E was found to be >1.5 μm (dashed line in Figure 6), which is larger than that of single quenching (∼0.6 μm), as we expected. Accordingly, the minimum R for satisfying A (= $2\gamma/ER$) < 0.5 (Figure 5d) increases with an increase of γ/E. In fact, the minimum R of buckling microgels for double quenching (12.5 μm) is larger than that of single quenching (7 μm). These tendencies support our theoretical model.

This spontaneous buckling resulting from the balance between the gel elasticity E and interfacial tension γ brings a new insight into the shape change of various elastic bodies with an inhomogeneous inner structure in the sol−gel coexisting phase, for example, microgels during polymerization (sol−gel transition)[20−23,27,28] and phase separation.[29,30] The buckling condition of the shell thickness ratio depending on the size of the elastic bodies and the characteristic size of γ/E derived from both experimental and theoretical analysis make it possible to apply spontaneous buckling for the morphological regulation of elastic bodies.

To focus on the condition of spontaneous buckling occurrence, we ignored the influence of core elasticity derived from the isolated domain of gelatin gel in the PEG solution. However, the core elasticity also becomes important, like shell elasticity and interfacial tension, in discussing the shape of buckling microgels (buckling mode). Compared to large microgels, small microgels tend to show a localized buckling with a large reduced volume (Figure 4a and Figure S3). It has been reported that as the elasticity ratio between the shell and core increases, the buckling depth increases and localized buckling tends to occur.[2,3,33] For small microgels where phase separation completes faster,[24] the core elasticity might be effectively reduced and finally lead to localized buckling. For a comprehensive understanding of the buckling pattern that is beyond the scope here, it will be necessary to consider the mechanical properties of the core depending on the microgel size.

CONCLUSION

We explored the influence of the inhomogeneous inner structure of microgels in a sol−gel coexisting phase on buckling by using core−shell microgels of a polymer solution that exhibits phase separation and gelation with a decrease in temperature. By preventing phase separation with gelation upon temperature quenching, we varied the shell thickness ratio h/R of the core−shell microgels. We found that the microgels with a certain h/R ratio spontaneously buckle without applying pressure. To explain this buckling condition of h/R, we analyzed the extended critical pressure for buckling by taking into account the gel elasticity E and interfacial tension between the sol−gel coexisting phase γ. The extended critical pressure is a downward-convex function with respect to the h/R ratio, which implies that the microgel having a certain h/R ratio at which the critical pressure reaches a minimum tends to buckle spontaneously. Moreover, the buckling condition of h/R depends on the ratio between the characteristic length γ/E and microgel radius R. The derived condition of spontaneous buckling contributes to establishing a method for microgel shape control through the inner structure in a sol−gel coexisting phase (e.g., emulsion polymerization).

ASSOCIATED CONTENT

Supporting Information

The Supporting Information is available free of charge on the ACS Publications website at DOI: 10.1021/acs.langmuir.8b03751.

Microscopic image of homogeneous microgels of gelatin (Figure S1), fluorescence image of microgels with different fluorescence localized in the gelatin-rich phase (Figure S2), and morphological analyses of buckling microgels (Figure S3) (PDF)

Buckling of microgels upon temperature decrease (Movie S1) (AVI)

Shape change of buckling microgels upon temperature increase (Movie S2) (AVI)

AUTHOR INFORMATION

Corresponding Author

*E-mail myanagisawa@g.ecc.u-tokyo.ac.jp (M.Y.).

ORCID

Miho Yanagisawa: 0000-0001-7872-8286

Notes

The authors declare no competing financial interest.

ACKNOWLEDGMENTS

We thank Prof. Masayuki Tokita (Kyushu University), Mr. Sinpei Nigorikawa (Kyushu University), and Mr. Atsushi Sakai (Tokyo University of Agriculture and Technology) for their experimental support in microgel preparation and Prof. Kei Fujiwara (Keio University) for critical reading of the manuscript. This work was supported by JSPS KAKENHI (M.Y.; No. 15KT0081, No. 16H01443, and No. 17H00769).

REFERENCES

(1) Chen, X.; Yin, J. Buckling patterns of thin films on curved compliant substrates with applications to morphogenesis and three-dimensional micro-fabrication. *Soft Matter* **2010**, *6* (22), 5667−5680.

(2) Yin, J.; Cao, Z.; Li, C.; Sheinman, I.; Chen, X. Stress-driven buckling patterns in spheroidal core/shell structures. *Proc. Natl. Acad. Sci. U. S. A.* **2008**, *105* (49), 19132−19135.

(3) Li, B.; Cao, Y. P.; Feng, X. Q.; Gao, H. J. Mechanics of morphological instabilities and surface wrinkling in soft materials: a review. *Soft Matter* **2012**, *8* (21), 5728−5745.

DOI: 10.1021/acs.langmuir.8b03751
Langmuir 2019, 35, 2283−2288

(4) Shim, J.; Perdigou, C.; Chen, E. R.; Bertoldi, K.; Reis, P. M. Buckling-induced encapsulation of structured elastic shells under pressure. *Proc. Natl. Acad. Sci. U. S. A.* **2012**, *109* (16), 5978−5983.
(5) Singamaneni, S.; Tsukruk, V. V. Buckling instabilities in periodic composite polymeric materials. *Soft Matter* **2010**, *6* (22), 5681−5692.
(6) Mei, H.; Huang, R.; Chung, J. Y.; Stafford, C. M.; Yu, H.-H. Buckling modes of elastic thin films on elastic substrates. *Appl. Phys. Lett.* **2007**, *90* (15), 151902.
(7) Mei, Y. F.; Kiravittaya, S.; Harazim, S.; Schmidt, O. G. Principles and applications of micro and nanoscale wrinkles. *Mater. Sci. Eng., R* **2010**, *70* (3−6), 209−224.
(8) Gao, L.; Zhang, Y. H.; Zhang, H.; Doshay, S.; Xie, X.; Luo, H. Y.; Shah, D.; Shi, Y.; Xu, S. Y.; Fang, H.; Fan, J. A.; Nordlander, P.; Huang, Y. G.; Rogers, J. A. Optics and Nonlinear Buckling Mechanics in Large-Area, Highly Stretchable Arrays of Plasmonic Nano structures. *ACS Nano* **2015**, *9* (6), 5968−5975.
(9) Chan, E. P.; Crosby, A. J. Fabricating microlens arrays by surface wrinkling. *Adv. Mater.* **2006**, *18* (24), 3238−3242.
(10) Chandra, D.; Yang, S.; Lin, P.-C. Strain responsive concave and convex microlens arrays. *Appl. Phys. Lett.* **2007**, *91* (25), 251912.
(11) Tallinen, T.; Chung, J. Y.; Rousseau, F.; Girard, N.; Lefevre, J.; Mahadevan, L. On the growth and form of cortical convolutions. *Nat. Phys.* **2016**, *12* (6), 588−593.
(12) Kim, D. H.; Rogers, J. A. Stretchable Electronics: Materials Strategies and Devices. *Adv. Mater.* **2008**, *20* (24), 4887−4892.
(13) Khang, D. Y.; Rogers, J. A.; Lee, H. H. Mechanical Buckling: Mechanics, Metrology, and Stretchable Electronics. *Adv. Funct. Mater.* **2009**, *19* (10), 1526−1536.
(14) Chung, J. Y.; Nolte, A. J.; Stafford, C. M. Surface Wrinkling: A Versatile Platform for Measuring Thin-Film Properties. *Adv. Mater.* **2011**, *23* (3), 349−368.
(15) Van der Heijden, A. M. *WT Koiter's Elastic Stability of Solids and Structures*; Cambridge University Press: Cambridge, England, 2008.
(16) Pan, B. B.; Cui, W. C. An overview of buckling and ultimate strength of spherical pressure hull under external pressure. *Mar Struct* **2010**, *23* (3), 227−240.
(17) Hutchinson, J. W. Imperfection sensitivity of externally pressurized spherical shells. *J. Appl. Mech.* **1967**, *34* (1), 49−55.
(18) Datta, S. S.; Kim, S. H.; Paulose, J.; Abbaspourrad, A.; Nelson, D. R.; Weitz, D. A. Delayed buckling and guided folding of inhomogeneous capsules. *Phys. Rev. Lett.* **2012**, *109* (13), 134302.
(19) Vernizzi, G.; Sknepnek, R.; Olvera de la Cruz, M. Platonic and Archimedean geometries in multicomponent elastic membranes. *Proc. Natl. Acad. Sci. U. S. A.* **2011**, *108* (11), 4292−6.
(20) Sacanna, S.; Irvine, W. T. M.; Chaikin, P. M.; Pine, D. J. Lock and key colloids. *Nature* **2010**, *464* (7288), 575−578.
(21) Sacanna, S.; Pine, D. J. Shape-anisotropic colloids: Building blocks for complex assemblies. *Curr. Opin. Colloid Interface Sci.* **2011**, *16* (2), 96−105.
(22) Shen, H. F.; Du, X. L.; Ren, X. L.; Xie, Y. H.; Sheng, X. X.; Zhang, X. Y. Morphology control of anisotropic nonspherical functional polymeric particles by one-pot dispersion polymerization. *React. Funct. Polym.* **2017**, *112*, 53−59.
(23) Yanagisawa, M.; Watanabe, C.; Fujiwara, K. Single Micrometer-Sized Gels: Unique Mechanics and Characters for Applications. *Gels* **2018**, *4* (2), 29.
(24) Yanagisawa, M.; Nigorikawa, S.; Sakaue, T.; Fujiwara, K.; Tokita, M. Multiple patterns of polymer gels in microspheres due to the interplay among phase separation, wetting, and gelation. *Proc. Natl. Acad. Sci. U. S. A.* **2014**, *111* (45), 15894−9.
(25) Yamashita, Y.; Yanagisawa, M.; Tokita, M. Sol-gel transition and phase separation in ternary system of gelatin-water-poly(ethylene glycol) oligomer. *J. Mol. Liq.* **2014**, *200*, 47−51.
(26) Yanagisawa, M.; Yamashita, Y.; Mukai, S.-A.; Annaka, M.; Tokita, M. Phase separation in binary polymer solution: Gelatin/poly (ethylene glycol) system. *J. Mol. Liq.* **2014**, *200*, 2−6.
(27) Salmon, A. R.; Parker, R. M.; Groombridge, A. S.; Maestro, A.; Coulston, R. J.; Hegemann, J.; Kierfeld, J.; Scherman, O. A.; Abell, C. Microcapsule Buckling Triggered by Compression-Induced Interfacial Phase Change. *Langmuir* **2016**, *32*, 10987.
(28) Park, S. H.; Kim, J.; Lee, W. E.; Byun, D. J.; Kim, M. H. One-Step Synthesis of Hollow Dimpled Polystyrene Microparticles by Dispersion Polymerization. *Langmuir* **2017**, *33* (9), 2275−2282.
(29) Bahadur, J.; Sen, D.; Mazumder, S.; Paul, B.; Bhatt, H.; Singh, S. G. Control of buckling in colloidal droplets during evaporation-induced assembly of nanoparticles. *Langmuir* **2012**, *28* (3), 1914−23.
(30) Pathak, B.; Basu, S. Phenomenology and control of buckling dynamics in multicomponent colloidal droplets. *J. Appl. Phys.* **2015**, *117* (24), 244901.
(31) Yamashita, Y.; Yanagisawa, M.; Tokita, M. Dynamics of Spinodal Decomposition in a Ternary Gelling System. *Gels* **2018**, *4* (2), 26.
(32) Sakai, A.; Murayama, Y.; Fujiwara, K.; Fujisawa, T.; Sasaki, S.; Kidoaki, S.; Yanagisawa, M. Increasing Elasticity through Changes in the Secondary Structure of Gelatin by Gelation in a Microsized Lipid Space. *ACS Cent. Sci.* **2018**, *4* (4), 477−483.
(33) Lagrange, R.; López Jiménez, F.; Terwagne, D.; Brojan, M.; Reis, P. M. From wrinkling to global buckling of a ring on a curved substrate. *J. Mech. Phys. Solids* **2016**, *89*, 77−95.

DOI: 10.1021/acs.langmuir.8b03751
Langmuir 2019, 35, 2283−2288